

## Theoretical Analysis of Mound Slope Selection during Unstable Multilayer Growth

Maozhi Li<sup>1</sup> and J. W. Evans<sup>2</sup>

<sup>1</sup>*Institute of Physical Research and Technology, and Ames Laboratory-USDOE, Iowa State University, Ames, Iowa 50011, USA*

<sup>2</sup>*Department of Mathematics, and Ames Laboratory-USDOE, Iowa State University, Ames, Iowa 50011, USA*

(Received 26 September 2005; published 13 December 2005)

A “step dynamics” model is developed for mound formation during multilayer homoepitaxy. Downward funneling of atoms deposited at step edges is incorporated and controls mound slope selection. Behavior of the selected slope differs from that predicted by phenomenological continuum treatments where the lateral mass current vanishes identically. Instead, this current is shown to vary periodically and vanish only on average. An exact coarse-grained continuum formulation with appropriate boundary conditions is derived and recovers step dynamics results.

DOI: [10.1103/PhysRevLett.95.256101](https://doi.org/10.1103/PhysRevLett.95.256101)

PACS numbers: 68.55.-a, 68.35.Fx, 81.10.Aj, 81.15.Aa

Atomistic models can provide a detailed description of structural or morphological evolution in materials and thin film systems. However, more direct insight into, e.g., long-time coarsening behavior, often comes from suitable coarse-grained formulations. Such formulations based on free energy minimization are available for Hamiltonian systems approaching equilibrium [1]. However, derivation of corresponding treatments for driven far-from-equilibrium systems often remains an open challenge in nonequilibrium statistical physics [2].

One important class of driven processes is kinetic roughening during multilayer homoepitaxial growth [3]. In such systems, initially two-dimensional (2D) islands are formed due to diffusion-mediated aggregation of atoms deposited on the substrate. The downward transport of atoms subsequently deposited on top of islands is typically inhibited by the presence of an additional step edge barrier [4]. Thus, diffusing atoms tend to be reflected from descending steps and incorporate at ascending steps. The resulting diffusion bias produces a net lateral mass current in the uphill direction, and results in unstable growth characterized by the formation of “mounds” (multilayer stacks of 2D islands) [5]. Once such mounds are formed, their sides tend to steepen. Additional nonthermal processes involving downward transport of atoms deposited near steps, e.g., downward funneling (DF) [6], counter this steepening, and eventually lead to slope selection [7,8]. This behavior has been explored via kinetic Monte Carlo simulation of atomistic lattice-gas models with emphasis on the slow coarsening of mound dimensions following slope selection [9,10].

Mound coarsening has also been analyzed extensively using phenomenological continuum treatments (PCT), in which the evolution of a continuous film height,  $h(x, t)$ , at lateral position  $x$  and time  $t$ , obeys [3,11–15]

$$\frac{\partial}{\partial t} h(x, t) = Fb - \nabla_x J_{\text{PCT}}(x, t). \quad (1)$$

Here  $F$  is the deposition flux in monolayer (ML) per unit time,  $b$  is the interlayer spacing, and  $J_{\text{PCT}}$  is the lateral mass current. Typically  $J_{\text{PCT}}$  is decomposed as  $J_{\text{PCT}} = J_{\text{DIFF}} + J_{\text{DF}} + J_{\text{SB}} + J_{\text{RELAX}}$ , where each term is propor-

tional to  $F$ , assuming no desorption and irreversible incorporation at step edges. Here  $J_{\text{DIFF}}(m)$  is the uphill current due to biased surface diffusion [3,5] depending on local slope  $m = \nabla_x h$  or terrace width  $L = b/|m|$ .  $J_{\text{DF}} \propto Fm$  is the downhill current due to downward funneling at step edges, which is proportional to step density (and thus to  $m$ ). The heuristic term  $J_{\text{SB}}$  produces up-down symmetry breaking, and  $J_{\text{RELAX}}$  facilitates “relaxation” near peaks and valleys [11,12]. Slope selection has been assumed to correspond to cancellation of uphill  $J_{\text{DIFF}}$  and downhill  $J_{\text{DF}}$  (noting that  $J_{\text{SB}}$  and  $J_{\text{RELAX}}$  vanish on straight mound sides). A noise term is often added to Eq. (1), but it is not important here.

In this Letter, we develop a step dynamics model to describe the evolution of steps in mound formation during unstable multilayer growth. In addition to inhibited interlayer transport, a key feature of our model is the incorporation of DF at step edges. Analysis of the evolution of a single mound reveals that slope selection occurs and is controlled by the boundary condition at the valley between mounds, which is in turn determined by the DF dynamics. The observed variation of the selected slope with diffusion bias is qualitatively distinct from behavior predicted by previous phenomenological continuum theories. The lateral mass current is found not to vanish identically (as assumed in PCT), but varies periodically and its total value over an entire mound side vanishes on average. An exact coarse-grained continuum theory is developed which recovers selected mound shapes. Our analysis provides a new understanding of mound shape and slope selection, including symmetry breaking and relaxation.

Previously, step dynamics models [12,16–18] were applied only for the evolution of mounds *without* DF or slope selection. However, DF is incorporated into our model, the basic ingredients of which are illustrated in Fig. 1 for the step-flow dynamics of a staircase representing a side of a  $(1+1)$ D mound. The mound valley is at  $x = 0$  and the peak is at  $x = R$ . The step  $n$  is located at  $x = x_n$ , where initially  $1 \leq n \leq n^*$ , so  $1 (n^*)$  labels the bottom (top) step. The width of the terrace  $n$  between step  $n$  and step  $n+1$  is  $L_n = x_{n+1} - x_n$ , for  $1 \leq n < n^*$ . The width of the bottom

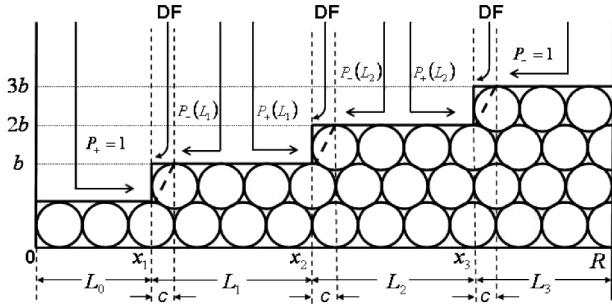


FIG. 1. Schematic of step dynamics model showing deposition, DF, and surface diffusion processes.  $x = 0$  ( $R$ ) denotes the mound valley (peak),  $x_i$  the position of step  $i$ , and  $L_i$  the width of terrace  $i$ .  $P_+$  ( $P_-$ ) gives the probability of diffusing to ascending (descending) steps. “Step edge regions” have width  $c$ .

(top) terrace is  $L_0 = x_1$  ( $L_{n^*} = R - x_{n^*}$ ). In our model, atoms deposited in a “step edge region” within a distance  $c$  above each step are funneled downward and incorporate at that step. All atoms deposited on the bottom (top) terrace aggregate to step 1 (step  $n^*$ ). Atoms deposited on terrace  $n$  ( $1 \leq n < n^*$ ) outside of the step edge region either aggregate to the ascending step  $n + 1$  with probability  $P_+(L_n)$ , or to the descending step  $n$  with probability  $P_-(L_n)$ . Here,  $P_+ + P_- = 1$ . The presence of a step edge barrier implies an uphill diffusion bias with strength  $P_+ - P_- = \Delta > 0$ . A specific form for  $P_{\pm}$  comes from solving the diffusion equation on each terrace with appropriate boundary conditions [3], but this form is not critical for our analysis, and we often set  $P_{\pm}$  constant. Finally, note that setting  $c = 0$  recovers a model without DF.

The total current of atoms reaching step  $n$  determines the velocity  $V_n$  of that step. Accounting for the different behavior indicated above for the bottom step,  $n = 1$ , steps in the interior of the staircase,  $1 < n < n^*$ , and the top step,  $n = n^*$ , one obtains

$$\frac{d}{dt}x_1 = V_1 = -FL_0 - F(L_1 - c)P_-(L_1) - Fc, \quad (2)$$

$$\begin{aligned} \frac{d}{dt}x_n = V_n = & -F(L_{n-1} - c)P_+(L_{n-1}) \\ & - F(L_n - c)P_-(L_n) - Fc, \end{aligned} \quad (3)$$

$$\begin{aligned} \frac{d}{dt}x_{n^*} = V_{n^*} = & -F(L_{n^*-1} - c)P_+(L_{n^*-1}) \\ & - F(L_{n^*} - c) - Fc. \end{aligned} \quad (4)$$

On the right-hand side of each equation, the first (second) term corresponds to diffusive current from the terrace to the left (right) of that step, and the third term is the DF current.

Evolution of the steps and terraces in mound formation can be analyzed by integrating the above equations with special treatments of the bottom steps (which disappear) and the top steps (which are nucleated). For the bottom step, Eq. (2) is only integrated until  $x_1$  reaches zero. At this time step 1 disappears, and step 2 becomes the bottom step.

So the equation for step 2 is updated from type Eq. (3) to type Eq. (2), then integrated until  $x_2$  reaches zero, etc. At the mound peak, new top layers are created by island nucleation. At a prescribed time of nucleation, we introduce a new step  $n^* + 1$  with position  $x_{n^*+1} = R$ , and update the equations appropriately. In our modeling, we primarily consider deterministic nucleation: a new top layer island is created when the width of the top terrace reaches some critical value,  $R_{\text{top}}$ .

One significant observation from Eqs. (2)–(4), is that for the evolution of the terrace width  $dL_n/dt = V_{n+1} - V_n$  ( $1 < n < n^*$ ), all terms including  $c$  (including DF terms) cancel out exactly for constant  $P_{\pm}$  (and approximately in general). Even so, DF will still dramatically influence mound shapes (as shown later), noting that DF terms persist in the evolution of the bottom and top terraces.

First, we investigate the existence of a selected slope and its behavior. For simplicity, initially we consider a semi-infinite mound  $n^* \rightarrow \infty$ . Here the effect of nucleation on step evolution is eliminated. It is found that irrespective of the initial choice of terrace width, the mound slope evolves to a unique selected value,  $m_s^{\infty}$ . For constant  $P_{\pm}$ , we find that  $m_s^{\infty} \approx 0.9b\Delta/c$  for smaller  $\Delta$ . We will provide detailed elucidation of this behavior elsewhere.

Next, we analyze the evolution of a mound with finite size. We apply deterministic nucleation at the mound peak. Figure 2 shows the mound shapes obtained from long-time solution of Eqs. (2)–(4), with constant  $P_+ = 0.52$  and  $c = 1/2$  (units of lattice constants) for various choices of  $R_{\text{top}}$ . Clearly, mound shapes are strongly influenced by the prescription of nucleation. However, for smaller  $R_{\text{top}}/R$ , a selected slope,  $m_s$ , develops which corresponds to that for the semi-infinite mound, i.e.,  $m_s = m_s^{\infty} \approx 1.8\Delta$  for  $c = 1/2$  and  $b = 1$ . Therefore, selected mound slopes are determined primarily by the evolution of the mound valley which is controlled by DF and diffusion bias.

We should emphasize that our result for the selected slope is qualitatively distinct from that of PCT. In the latter, the selected slope  $m_s^{\text{PCT}}$  was obtained by balancing the

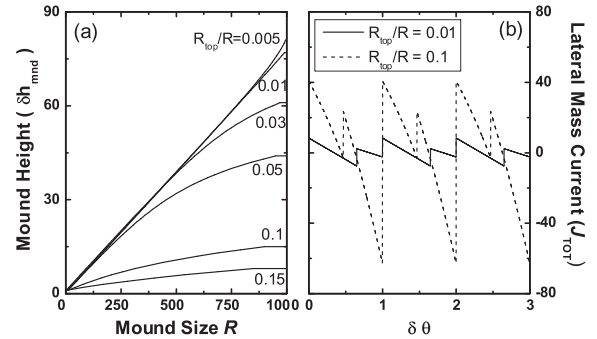


FIG. 2. (a) Selected mound shapes for various choices of  $R_{\text{top}}$  for nucleation; (b) periodic variation of the total mass current,  $J_{\text{TOT}}$ , with coverage increment,  $\delta\theta$ , for different  $R_{\text{top}}$ .  $\delta\theta = 0$  corresponds to top layer nucleation. Here  $P_+ = 0.52$ ,  $c = 1/2$ ,  $b = 1$ , and  $R = 1000$ .

magnitudes of uphill current  $J_{\text{DIFF}} \approx (1/2)Fb^2\Delta/m$ , and downhill current  $J_{\text{DF}} \approx -Fc^2m/2$  [8], so that  $m_s^{\text{PCT}} \approx b\sqrt{\Delta}/c$ . Figure 3 highlights the discrepancy between this nonlinear dependence on  $\Delta$  and the quasilinear dependence from the step dynamics model.

In order to explain this discrepancy, it will be instructive to analyze the total lateral mass current,  $J_{\text{TOT}}$ , across the side of the mound between its valley and peak. We now identify the different contributions. The net diffusive current across the terrace  $n$  for  $1 \leq n < n^*$ ,  $J_n = +F(L_n - c)[P_+(L_n) - P_-(L_n)] > 0$ , is uphill. The current across the bottom terrace where all atoms reach step 1,  $J_0 = +FL_0 > 0$ , is also uphill. In contrast, the current across the top terrace,  $J_{n^*} = -F(L_{n^*} - c) < 0$ , is downhill. In addition, there is a downhill current from DF of  $J_{\text{df}} = -Fc$  at each step. For constant  $P_{\pm}$ , the total lateral mass current is simply given by

$$J_{\text{TOT}}/F = \Delta R + 2P_-x_1 - 2P_+L_{n^*} - 2P_+c(n^* - 1). \quad (5)$$

The long-time solution to Eqs. (2)–(4), is not time invariant, but rather periodic (in the moving reference frame) with period of one monolayer (ML). Thus,  $J_{\text{TOT}}$  varies periodically as shown in Fig. 2(b). Just after nucleation of a top layer island, downhill contribution from the top terrace is almost zero. Also, the net uphill current on other terraces dominates the DF current, so  $J_{\text{TOT}}$  is positive. As the top terrace grows, the downhill current across it grows and subsequently dominates the uphill contributions, so  $J_{\text{TOT}}$  becomes negative until a new layer is created (when a new period begins). The small jump in each period corresponds to the disappearance of the bottom step. Our *key finding* is that the mean value of  $J_{\text{TOT}}$  averaged over one ML always vanishes (when  $c > 0$ ). This is qualitatively different from the simplistic picture of phenomenological theory where the lateral current is assumed to vanish identically on mound sides, and causes the distinct behavior found for the selected slope.

Next, we provide a further illustration that slope selection depends critically on DF to the mound valley by

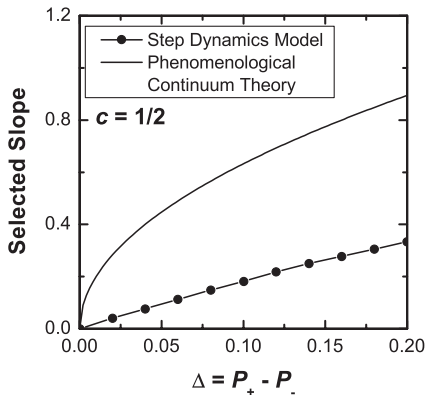


FIG. 3. Comparison of the behavior of the selected slope with  $\Delta$  obtained from step dynamics model and the phenomenological continuum theory for  $b = 1$ .

analyzing the evolution of a mound *without* DF ( $c = 0$ ). We find that a deep groove develops at the mound valley either for a semi-infinite mound, or for a finite mound (if  $R_{\text{top}}$  is not too large). This corresponds to the mound valley advancing upwards relatively slowly. This behavior is self-evident in the extreme case with no interlayer transport ( $P_+ = 1$ ), since the bottom step never disappears without DF.

In addition, we have systematically analyzed the evolution of a finite mound *without* DF ( $c = 0$ ). For  $P_+ = 0.55$ , a deep groove develops if  $R_{\text{top}}/R < 0.21$  [cf. Zeno Model [12]]. Furthermore, one finds progressive roughening and the mean value of  $J_{\text{TOT}}$  over a period of one ML is positive. On the contrary, if  $R_{\text{top}}/R > 0.21$ , the mound evolves to a stationary shape, and the mean value of  $J_{\text{TOT}}$  over one ML vanishes. Now there is no DF, so the negative contribution to  $J_{\text{TOT}}$  comes entirely from diffusion across the top terrace. We note that although a stationary shape is obtained, there is no tendency for slope selection without DF.

Finally, given the shortcomings of the phenomenological continuum treatment, we are motivated to derive an exact continuum formulation starting from our discrete step dynamics equations. One strategy assumes that a continuous smooth function  $h = h(x, t)$  is fit through the vertically discrete step edges [17,18], so that  $h(x_{n+1}, t) - h(x_n, t) \approx b$  for each  $n$ . Then, the desired evolution equation follows using

$$\frac{\partial}{\partial t} h(x_n, t) \approx -V_n \frac{\partial}{\partial x} h(x_n, t). \quad (6)$$

To determine the explicit form of the right-hand side of this equation, we use a Taylor expansion to obtain

$$h(x_{n+1}) - h(x_n) = L_n h_x(x_n) + L_n^2 h_{xx}(x_n)/2 + \dots (= b). \quad (7)$$

Equation (7) can be solved for  $L_n$  in terms of the local terrace width  $L(x) = b/h_x$  (for  $h_x > 0$ ) to obtain

$$L_n \approx L(x) + L(x)L_x(x)/2 + L(x)[L(x)L_x(x)]_x/6 + \dots \quad (8)$$

(dropping the  $t$  dependence). For  $L_{n-1}$ , one obtains the same expression but with a sign change in the second term. Substituting Eq. (8) for  $L_n$  and  $L_{n-1}$  into Eqs. (3) and (6), and expanding  $P_-(L_n)$  and  $P_+(L_{n-1})$  in Eq. (3) about  $L(x)$ , finally one obtains

$$\frac{\partial}{\partial t} h(x, t) \approx Fb - \frac{\partial}{\partial x} J_{\text{EXACT}}, \quad (9)$$

where  $J_{\text{EXACT}} = Fb\Delta(L - c)/2 - FbLL_x/6$ . Our derivation of Eq. (9) holds for general  $P_{\pm}$ , subject to the constraint of  $P_+ + P_- = 1$ . The second term in  $J_{\text{EXACT}}$  breaks up-down symmetry. Apart from its coefficient, our result is consistent with that from a direct analysis of steady-state behavior just for  $c = 0$  (no DF) in Ref. [12].

The steady-state solution of Eq. (9) for  $\delta h = h - Fbt$  can be obtained by solving  $J_{\text{EXACT}} = \text{const}$ . This gives a

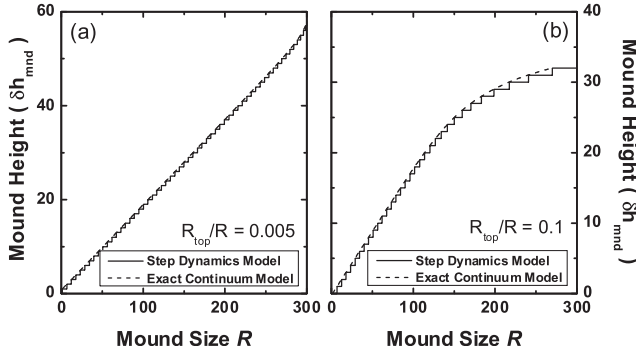


FIG. 4. Comparison of the selected mound shapes obtained from step dynamics model and the exact continuum Eq. (9).  $P_+ = 0.55$ ,  $c = 1/2$ ,  $b = 1$ , and  $R = 300$ . (a)  $R_{\text{top}}/R = 0.005$ ; (b)  $R_{\text{top}}/R = 0.1$ .

first-order equation for the local slope  $m(x, t) = h_x(x, t) = b/L(x, t)$  and involves an unknown constant. We must keep the second higher-order term in  $J_{\text{EXACT}}$  to avoid a trivial solution,  $m = \text{const}$ . Two boundary conditions are required to solve this equation. The first comes from matching the correct selected slope at the mound valley. The second derives from a simplified version of the constraint on  $J_{\text{TOT}}$ . Specifically, we assume that  $J_{\text{TOT}}$  vanishes when the top terrace width satisfies  $L_{n^*} = \alpha R_{\text{top}}$  for suitable  $\alpha$  around  $1/2$ . This yields a value for the mound height [19]

$$\delta h_{\text{mnd}}/b = 1 + [\Delta R + P_-(2\Delta) - 2\alpha P_+ R_{\text{top}}]/(2P_+ + c). \quad (10)$$

Equation (10) imposes a mound height consistent with our specification of nucleation. Figure 4 shows that this continuum formulation successfully recovers the nontrivial mound shapes from our step dynamics analysis choosing  $\alpha$  based on numerical results for  $J_{\text{TOT}}$ .

As an aside, using a different approach, we have also obtained an exact Fokker-Planck type equation for the terrace width distribution,  $L(h, t)$ , as a function of height,  $h$  [20]. We find that this equation also recovers observed mound shapes if one retains higher-order terms. We also note that Eq. (6) is utilized in Ref. [21] where it facilitates coarse graining of step dynamics modeling.

Comparing Eq. (9) with Eq. (1),  $J_{\text{EXACT}}$  in Eq. (9) contains no DF or relaxation components. Slope selection using Eq. (9) comes not from an explicit DF term in  $J_{\text{EXACT}}$ , but rather from the boundary condition at the mound valley. Relaxation at the peak comes from imposition of Eq. (10). Symmetry breaking derives from the explicit term in  $J_{\text{EXACT}}$ , and from the different nature of the boundary conditions at the mound valley and peak.

Can one develop a reliable phenomenological continuum equation, replacing the boundary condition at the mound peak with a relaxation term? This may be viable with a more realistic prescription of nucleation [3]:

when the top layer island has radius  $R_{\text{isl}}$ , the probability of nucleation has the form  $P_{\text{nuc}}(R_{\text{isl}}) \sim (R_{\text{isl}})^{n-1} \times \exp[-c_n(R_{\text{isl}}/R_{\text{top}})^n]$ . When implemented in Eqs. (2)–(4), we find the shape of the mound peak becomes smooth after averaging over many ML of deposition. Now  $J_{\text{TOT}}$  does not vanish when averaged over a single ML, but will when averaged over many ML. This smooth shape might be described by a continuum equation including a relaxation term which produces a downhill current near the mound peak, and reflects an average of the downhill diffusive current across the top of a mound.

In conclusion, our analysis of the mound shapes and slope selection in homoepitaxial growth produces a qualitatively different picture from the commonly accepted phenomenological continuum theory. Numerical results were shown just for the case of constant  $P_{\pm}$ , but our conclusions hold more generally. This study develops a foundation for more rigorous and reliable treatments of unstable growth phenomenon.

This work was supported by NSF Grant No. CHE-0414378, performed at Ames Laboratory-USDOE which is operated under Contract No. W-7405-Eng-82, and motivated by discussions with R. V. Kohn.

- 
- [1] A. J. Bray, *Adv. Phys.* **43**, 357 (1994).
  - [2] A. L. Barabasi and H. E. Stanley, *Fractal Concepts in Surface Growth* (Cambridge University Press, Cambridge, England, 1995).
  - [3] T. Michely and J. Krug, *Islands, Mounds and Atoms* (Springer, New York, 2004).
  - [4] G. Ehrlich and F. G. Hudda, *J. Chem. Phys.* **44**, 1039 (1966).
  - [5] J. Villain, *J. Phys. I (France)* **1**, 19 (1991).
  - [6] J. W. Evans *et al.*, *Phys. Rev. B* **41**, R5410 (1990).
  - [7] M. C. Bartelt and J. W. Evans, *Phys. Rev. Lett.* **75**, 4250 (1995).
  - [8] J. G. Amar and F. Family, *Phys. Rev. B* **54**, 14 071 (1996).
  - [9] P. Smilauer and D. D. Vvedensky, *Phys. Rev. B* **52**, 14 263 (1995).
  - [10] J. G. Amar, *Phys. Rev. B* **60**, R11317 (1999).
  - [11] J. A. Stroschio *et al.*, *Phys. Rev. Lett.* **75**, 4246 (1995).
  - [12] P. Politri and J. Villain, *Phys. Rev. B* **54**, 5114 (1996).
  - [13] M. Siegert, *Phys. Rev. Lett.* **81**, 5481 (1998).
  - [14] L. Golubovic, A. Levandovsky, and D. Moldovan, *Phys. Rev. Lett.* **89**, 266104 (2002).
  - [15] A. Levandovsky and L. Golubovic, *Phys. Rev. B* **69**, 241402(R) (2004).
  - [16] J. Krug, *Physica (Amsterdam)* **313A**, 47 (2002).
  - [17] W. E. and N. K. Yip, *J. Stat. Phys.* **104**, 221 (2001).
  - [18] R. V. Kohn, T. S. Lo, and N. K. Yip, *MRS Proc.* **696**, T1.7 (2002).
  - [19] We have set  $x_1 = \beta L(x = 0)$ , i.e., a fraction of the selected terrace width, and chosen  $\beta = 1/2$ .
  - [20] M. Li and J. W. Evans (to be published).
  - [21] N. Israeli and D. Kandel, *Phys. Rev. Lett.* **88**, 116103 (2002).